Since January 2020 Elsevier has created a COVID-19 resource centre with free information in English and Mandarin on the novel coronavirus COVID-19. The COVID-19 resource centre is hosted on Elsevier Connect, the company's public news and information website.

Carbohydrate Polymers 248 (2020) 116737

Contents lists available at ScienceDirect

Carbohydrate Polymers

journal homepage: www.elsevier.com/locate/carbpol

Isolation and characterization of an exopolymer produced by *Bacillus licheniformis*: *In vitro* antiviral activity against enveloped viruses

E. Sánchez-León[a,1], R. Bello-Morales[a,b,1], J.A. López-Guerrero[a,b], A. Poveda[c], J. Jiménez-Barbero[c,d], N. Gironès[a,b], C. Abrusci[a,b,*]

[a] Departamento de Biología Molecular, Facultad de Ciencias, Universidad Autónoma de Madrid, UAM, Cantoblanco, 28049, Madrid, Spain
[b] Centro de Biología Molecular Severo Ochoa, CSIC-UAM, Madrid, Spain
[c] CIC bioGUNE, Basque Research and Technology Alliance-BRTA, Parque Científico Tecnológico de Bizkaia, 48160, Derio, Biscay, Spain
[d] Ikerbasque, Basque Foundation for Science, 48009, Bilbao, Biscay, Spain

ARTICLE INFO

Keywords:
Bacillus licheniformis
Poly(γ-glutamic acid)
Teichoic acids
Antiviral
Enveloped viruses

ABSTRACT

The exopolymer (EPSp) produced by the strain *B. licheniformis* IDN-EC was isolated and characterized using different techniques (MALDI-TOF, NMR, ATR-FTIR, TGA, DSC, SEM). The results showed that the low molecular weight EPSp contained a long polyglutamic acid and an extracellular teichoic acid polysaccharide. The latter was composed of poly(glycerol phosphate) and was substituted at the 2-position of the glycerol residues with a αGal and $\alpha GlcNH_2$. The αGal O-6 position was also found to be substituted by a phosphate group. The antiviral capability of this EPSp was also tested on both enveloped (herpesviruses HSV, PRV and vesicular stomatitis VSV) and non-enveloped (MVM) viruses. The EPSp was efficient at inhibiting viral entry for the herpesviruses and VSV but was not effective against non-enveloped viruses. The *in vivo* assay of the EPSp in mice showed no signs of toxicity which could allow for its application in the healthcare sector.

1. Introduction

The rapid appearance of microorganisms that can cause zoonotic diseases can cause severe health problems as, due to their sudden emergence, there typically are no vaccines available to counteract them. In the last two decades, two novel zoonotic viruses have emerged causing fatal epidemics in humans: the severe acute respiratory syndrome coronavirus (SARS-CoV), and the Middle East (MERS-CoV), which appeared in 2002 and 2012 respectively. Most recently, the SARS-CoV-2 (Gorbalenya et al., 2020) has been the causal agent for the coronavirus pandemic (COVID-19) which has posed a serious threat to global health and economy. In the cases where the mechanisms of action of the pathogen are not well known, these can lead to the collapse of whole countries' health systems. It is therefore necessary to research and implement antiviral compounds that have effects on a broader spectrum in order to prevent and combat possible pandemics. This type of antiviral treatments can effectively and rapidly reduce infection rates (Harrison, 2020)

These antiviral compounds can be obtained through biotechnological processes undertaken by microorganisms that can adapt to different environments. This is the case of bacteria that can produce and secrete extracellular polymeric substances (EPS) with a highly heterogeneous composition (More, Yadav, Yan, Tyagi, & Surampalli, 2014; Rehm, 2010). These compounds play a role in the protection against desiccation, predation by protozoans and viruses and in the survival in nutrient-starved environments (Panosyan, Di Donato, Poli, & Nicolaus, 2018). These polymers' attributes have led to their use in a wide range of applications in different industrial sectors (Ates, 2015; Donot, Fontana, Baccou, & Schorr-Galindo, 2012). Their antimicrobial properties have been the focus of past research (Yu, Shen, Song, & Xie, 2018) and, in particular, several studies have reported the antiviral effect on several viruses. These include herpes simplex type 1 (HSV-1) (Gugliandolo et al., 2015; Marino-Merlo et al., 2017), herpes simplex type 2 (HSV-2) (Arena et al., 2006), encephalomyocarditis virus (EMCV) (Yim et al., 2004), influenza virus (Zheng, Chen, Cheng, Wang, & Chu, 2006), infectious hematopoietic necrosis virus (IHNV) and infectious pancreatic necrosis virus (IPNV) (Nácher-Vázquez et al., 2015).

The lack of efficient drugs to treat fast emerging pandemics makes it imperative to speed up the research for antiviral agents that are effective against future viral threats. This study reports the finding of a novel

* Corresponding author at: Departamento de Biología Molecular, Facultad de Ciencias, Universidad Autónoma de Madrid, UAM, Cantoblanco, 28049, Madrid, Spain.
E-mail address: concepcion.abrusci@uam.es (C. Abrusci).
[1] Equal contribution.

https://doi.org/10.1016/j.carbpol.2020.116737
Received 29 April 2020; Received in revised form 19 June 2020; Accepted 3 July 2020
Available online 08 July 2020
0144-8617/

EPSp composed of Poly-γ-glutamic acid and an extracellular teichoic acid polysaccharide (Birch, Van Calsteren, Pérez, & Svensson, 2019). This EPSp was isolated and characterized from *B. licheniformis* and it was found to exhibit a drastic inhibitory activity in cell cultures against multiple human and animal viruses. The EPSp was applied to four enveloped viruses (HSV-1 and HSV-2 which infect humans and PRV and VSV which infects animals); and a non-enveloped virus (MVM) that infects animals. In particular, the EPS was most effective when used against enveloped viruses as it significantly reduced the viral yield. This EPSp has been proven to be non-toxic in mice and, given its potent antiviral capability *in vitro*, it is proposed as a good candidate for further studies in cell cultures with other enveloped viruses and potentially in animal models, in order to establish its efficacy *in vivo* against enveloped viral infection.

2. Materials and methods

2.1. Chemicals and standards

The anti-HSV gD LP2 antibody was sourced from Alexa555, conjugated secondary anti-mouse and anti-rabbit antibodies were sourced from Molecular Probes (Eugene, OR, USA), and Mowiol was obtained from Calbiochem (Merck Chemicals, Germany). The rest of reagents were purchased from Sigma Chemical Co. (St. Louis, MO, USA).

2.2. Bacterial strain

The indigenous bacterial strain, *Bacillus licheniformis* IDN-EC, had been isolated from films based on Poly(Butylene Adipate-co-Terephthalate) and its blend with Poly (Lactic Acid) (Morro, Catalina, Sanchez-León, & Abrusci, 2019).

2.3. Production of exopolymer

Bacillus licheniformis IDN-EC was inoculated from the stock culture in trypticase soya agar medium (TSA) and incubated at 45 °C for 24 h. After that, the strains were transferred into flasks of 100 ml filled with 20 ml of minimal growth medium (MGM), prepared as described by Abrusci et al. (2011).: g/L: K_2HPO_4 0.5, KH_2PO_4 0.04, NaCl 0.1, $CaCl_2$ $2H_2O$ 0.002, (NH_4) $2SO_4$ 0.2, $MgSO_4$ $7H_2O$ 0.02, $FeSO_4$ 0.001, and glucose as a carbon source at a concentration of 4 g/L, pH adjusted to 7.0. The flasks were incubated in a rotary shaker incubator (Biogen) at 45 °C and 110 rpm for 24 h. After the first incubation, 10 ml of this broth (2.5×10^7 cells/mL concentration) was inoculated into flasks of 1000 ml filled with 100 ml of MGM with glucose supplementation. The flasks were incubated at 45 °C and 110 rpm for 48 h, when the stationary phase was reached. Three independent assays were performed.

2.4. Biodegradation, cell growth, and pH

The biodegrading bacteria were evaluated by indirect impedance measurements. The aerobic biodegradation of glucose compound by *B. licheniformis* was performed at 45 °C. The bioassays were carried out in bioreactors of 7 ml, filled with 1.5 mL of bacterial suspension prepared as described above. These containers were introduced into disposable cylindrical cells of 20 mL filled with 1.5 mL of 2 g/L KOH aqueous solution and provided by four stainless steel electrodes to measure impedance on a Bac-Trac 4300 apparatus (SY-LAB Geräte GmbH, Neupurkerdorf, Austria). The method has a typical error in the measurements of 1–2 %. The experimental device and procedure have been previously described in the literature (San Miguel, Peinado, Catalina, & Abrusci, 2009). The device monitors the relative change (each 20 min) in the initial impedance value of KOH solution, which is converted in concentration of carbon dioxide by a calibration curve of impedance variation versus concentration of CO_2. The percentage of biodegradation of glucose was calculated as a percentage of the ratio between the cumulative amount of CO_2 produced in the biodegradation at time, t, and the theoretical amount of carbon dioxide assuming that all the carbon of the glucose structures introduced in the bioreactor are transformed into CO_2. % Biodegradation = ($[CO_2]$Prod/$[CO_2]$Theor.) × 100.

The cell growth number was evaluated by different dilution plating incubated at 45 °C for 48 h with TSA agar medium. A Thermo Orion pH Meter (model, 2 Star) was used to determine the pH values during a fermentation period of 48 h.

2.5. Isolation and purification of the EPS

The cultures obtained from the strain *B. licheniformis* IDN-EC were centrifuged at 13,154 × g for 30 min at 4 °C (Duppont - RC5). The EPS was precipitated with cold ethanol (three times the volume) and left overnight. The precipitate was collected by centrifugation at 13,154 × g for 30 min at 4 °C and dissolved in Milli-Q water. Then the crude EPS was dialyzed at 4 °C with Milli-Q water for 48 h. The dialyzed contents were then freeze dried by lyophilization for 48 h and the dry weight of the powdered EPS was determined.

The further purification of crude EPS (10 mL, 10 mg/mL) was subjected to a DEAE-52 anion exchange column (2.6 × 30 cm) and eluted with deionized water, 0.05 and 0.3 M NaCl at 1 mL/min flow rate.

2.6. Mass spectrometry

MALDI-TOF mass spectra were recorded on an Ultraflex III TOF/TOF mass spectrometer (BrukerDaltonics) equipped with a Nd:YAG laser (355 nm). Mass spectra were recorded in positive reflector (range 1–10 KDa) and lineal (range 1–20 KDa) modes, using a matrix of 10 mg/mL 2,5-dihydroxibenzoic acid (DHB) in methanol/water (90/10).

2.7. Monosaccharide analysis

To determine the monosaccharide composition, the EPSp was hydrolyzed with trifluoroacetic acid (TFA) 0.5 M at 120 °C for 2 h. The samples were treated before and after the process with N_2. The monosaccharide content of EPSp was analyzed by HPLC using a 920LC Varian apparatus equipped with a PL-EDS 2100 Ice detector. A sugar SP0810 (Shodex) column as a stationary phase was used with an isocratic mobile phase of water as a solvent and a flow rate of 0.5 mL/min. The column temperature was maintained at 30 °C. The samples injection volume was 50 μL. The monosaccharide such as glucose, arabinose, rhamnose, xylose, mannose, galactose, fructose and sorbose were used as standards. The concentration of glucuronic acid was determined by HPLC/MSMS using an Agilent Technologies 1100 series - 6410B (TQ). An ACE Excel 3 C18-Amide column as a stationary phase was used with a mobile phase of 0.1 % formic acid in water. Flow rate of 0.2 ml/min. The temperature for analysis was set at 40 °C.

2.8. NMR spectroscopy

For NMR sample preparation, *ca* 4 mg of the EPSp sample were dissolved in 0.5 ml of deuterated water D_2O. NMR spectra were acquired using either a Bruker AVIII-600 spectrometer equipped with a 5 mm PATXI 1 H/D-13C/15 N XYZ-GRD probe (for ^1H and ^{13}C experiments) or a 5 mm QXI 1H XYZ-GRD probe (for ^1H and ^{31}P experiments), or in a Bruker AVIII-800 equipped with a cryoprobe 5 mm CPTCI 1H-13C/15 N/D Z-GRD. All experiments were recorded using standard Bruker pulse sequences and the temperature was set at 298 K. Chemical shifts are expressed in parts per million (δ, ppm) with respect to the 0 ppm point of DSS (4-dimethyl-4-silapentane-1-sulfonic acid), used as an internal standard.

The composition of the sample and the structure of the compounds was determined using a combination of 1D (^1H, 1D-selective TOCSY,

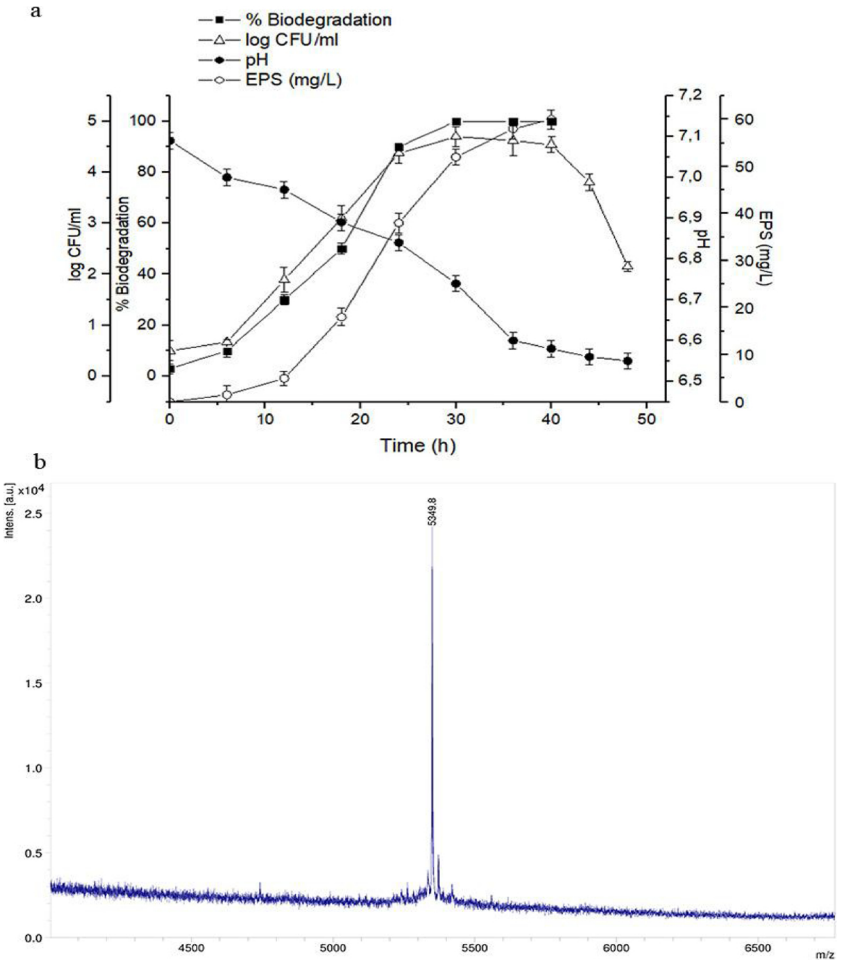

Fig. 1. Characterization of the exopolymer EPSp extracted from *B. licheniformis* IDN-EC. a) Time course of glucose biodegradation, colony-forming unit (CFU), pH value, and EPSp production at 45 °C over time from 0 to 48 h. b) MALDI-TOF mass spectroscopy of EPSp.

Table 1
δ_H, δ_C and δ_P values (ppm) obtained from the analysis of the ^{1}H-^{13}C HSQC and HMBC NMR experiments.

	CH(α)	CH_2(β)	CH_2(γ)	CO(α)	CO(γ)	
γ-Poly Glutamic Acid	4.1 57.5	2.1, 1.9 30.4	2.4 34.9	 180.0	 177.8	
		CH_2(1)	CH(2)	CH_2(3)		$^{31}P^{(a)}$
PolyGlycerol [1,2] type: R1 = PO_3, R2 = Gal, R3 = H		4.1, 4.0 67.1	3.9 80.0	3.8 63.9		3.48
PolyGlycerol [1,3] type: R1 = PO_3, R2 = H, R3 = PO_3		3.9 68.8	4.1 72.1	3.9 68.8		3.15, 3.26
PolyGlycerol [1,2,3] type: R1 = PO_3, R2 = GlcN, R3 = PO_3		4.0 67.8	4.1 78.4	4.0 67.8		3.48
	CH(1)	CH(2)	CH(3)	CH(4)	CH(5)	CH_2(6)	$^{31}P^{(a)}$
αGal	5.2 101.2	3.8 71.0	3.9 71.8	4.0 71.6	4.3 72.5	4.0 67.3	3.48
αGlcN	5.1 99.4	3.9 56.3	3.7 73.7	3.5 72.7	3.9 74.7	3.9, 3.8 63.2	

[a]There are three groups of signals in the ^{31}P spectra at δ_P 3.15, 3.26, and 3.48 ppm that correlate with the corresponding CH_2 groups in the ^{1}H-^{31}P HMBC NMR spectrum.

NOESY and ROESY experiments) and 2D (DOSY, COSY, ^{1}H-^{13}C-HSQC, ^{1}H-^{13}C-HSQC-TOCSY, ^{1}H-^{31}P-HMBC) NMR experiments. For the ^{1}H-^{13}C -HSQC experiment, values of 10 ppm and 2 K points, for the ^{1}H dimension, and 90 ppm and 256–512 points for the ^{13}C dimension, were used. For the homonuclear COSY experiment, 8 ppm windows were used with a 1 K x 256-point matrix. For the 1D-selective NOESY experiments, mixing times of 300 ms were used. For the 1D-selective ROESY experiments spinlock times of 300 ms were also used. For the HSQC-TOCSY mixing times of 80 ms were used, while for the 1D- selective version 30 − 100 ms range was used. For the ^{1}H-^{31}P-HMBC and ^{1}H-^{31}P-HSQMBC-TOCSY experiments, values of 4 − 10 ppm and 2 K points, for the ^{1}H dimension, and 8 − 40 ppm and 128–256 points for

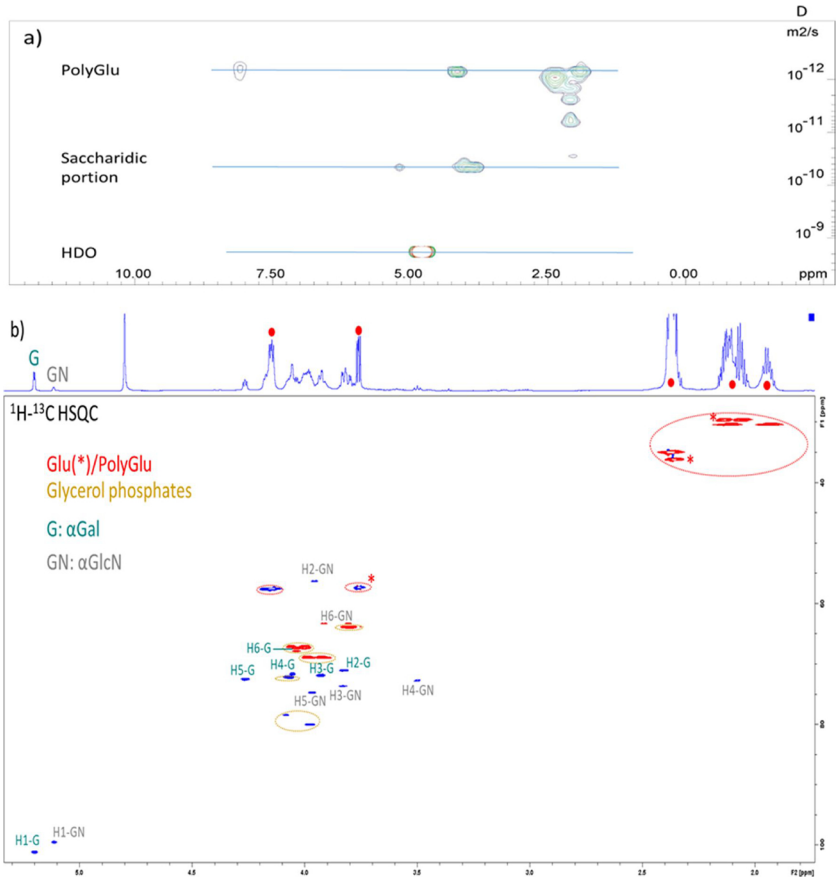

Fig. 2. Nuclear magnetic resonance (NMR) analysis of the exopolymer EPSp. a) DOSY NMR experiment showing the presence of two components in the mixture with different diffusion coefficient times and therefore, different molecular weights. b) ^{1}H-^{13}C HSQC NMR spectrum showing the signals assignment of the diverse molecules in the sample.

the ^{31}P dimension, were used. These experiments were optimized for a long-range coupling constant of 10 Hz, and 40 ms were used as mixing time for the TOCSY version. The DOSY experiment was acquired using the ledbpgp2s pulse sequence from the Bruker library. An exponential gradient list of 24 values was created by using the standard AU program dosy. Experiments were acquired using 8 scans, $\delta/2$ of 1.8 ms, diffusion time Δ of 500 ms, and eddy current delay value of 5 ms.

2.9. Attenuated total reflectance/FT-infrared spectroscopy (ATR/FTIR). Thermogravimetric analysis

The structural-functional groups of the EPSp were detected using Attenuated Total Reflectance/FT-Infrared Spectroscopy (ATR-FTIR). IR spectra were obtained using a Perkin Elmer BX-FTIR spectrometer coupled with an ATR accessory, MIRacleTM-ATR from PIKE Technologies and interferograms were obtained from 32 scans at a 4 cm^{-1} with a resolution from 400 to 4000 cm^{-1}.

Thermogravimetric analysis (TGA) of the polymer was done using a TGA Q-500 (Perkin-Elmer). The heating rate for the dynamic conditions was 10 °C/min, and the nitrogen flow was maintained constant at 60 mL/min.

2.10. Scanning electronic microscopy (SEM)

Scanning electronic microscopy micrographs were obtained using a Philips XL 30 scanning electron microscope operating in conventional high-vacuum mode at an accelerating voltage of 25 kV. Previously, EPSp was coated with a 3 nm thick gold/palladium layer.

2.11. Cell lines and viruses

Vero, HOG, MeWo and Hela cell lines were propagated in DMEM supplemented with 10 % FBS, penicillin (50 U/mL) and streptomycin (50 µg/mL) at 37 °C in an atmosphere of 5 % CO_2, (Bello-Morales et al., 2012). The Jurkat cell line was cultured in RPMI 1640 medium supplemented with 10 % FBS, 2 mM glutamine, 1 mM sodium pyruvate, 10 mMHepes, and 100 mg/mL each of penicillin and streptomycin as described (Alonso, Mazzeo, Mérida, & Izquierdo, 2007).

In this study, HSV-1 K26GFP (Desai & Person, 1998), HSV-2, PRV XGF-N (Viejo-Borbolla, Muñoz, Tabarés, & Alcamí, 2010), VSV-GFP and MVM viruses were tested. Herpesviruses were propagated and titrated on Vero cells. VSV-GFP and MVM viruses were propagated and titrated on Hela cells. The virus HSV-1 (KOS) gL86, a β-galactosidase–expressing version of KOS strain (Montgomery, Warner, Lum, & Spear, 1996), was used to monitor the viral entry.

2.12. Viral infection methodology

To evaluate the effect of EPSp on viral infections, cells were plated in 24-well plates, with or without glass coverslips and, 24 h later, confluent monolayers were infected with a mixture of viruses and EPSp. The control virus (W/O) and the EPSp treated virus (EPSp) was prepared. To prepare the amount necessary for 10 wells and a 5 µg/mL concentration, the virus was incubated at a m.o.i. of 0.5 $TCID_{50}$/mL in a microcentrifuge tube with 10 µl of EPSp mg/mL (1 µl of EPSp per well) in serum-free DMEM as part of a pre-treatment prior to cell infection. The final volume was then adjusted to 30 µl and left in the tube for 1 h at 37 °C in a CO_2 incubator. After that, 2 ml of serum-free DMEM was added to the tube containing the viral inoculum and EPSp. The cells were washed with serum-free DMEM, and infected with 200 µl per well of the viral inoculum and EPSp mixture resulting in a final EPSp concentration of 5 µg/mL. After 1 h of viral adsorption, the inoculum was withdrawn and the cells were washed twice with serum-free DMEN. Finally, cells were incubated in DMEM 10 % FBS for 24 h. The effect of

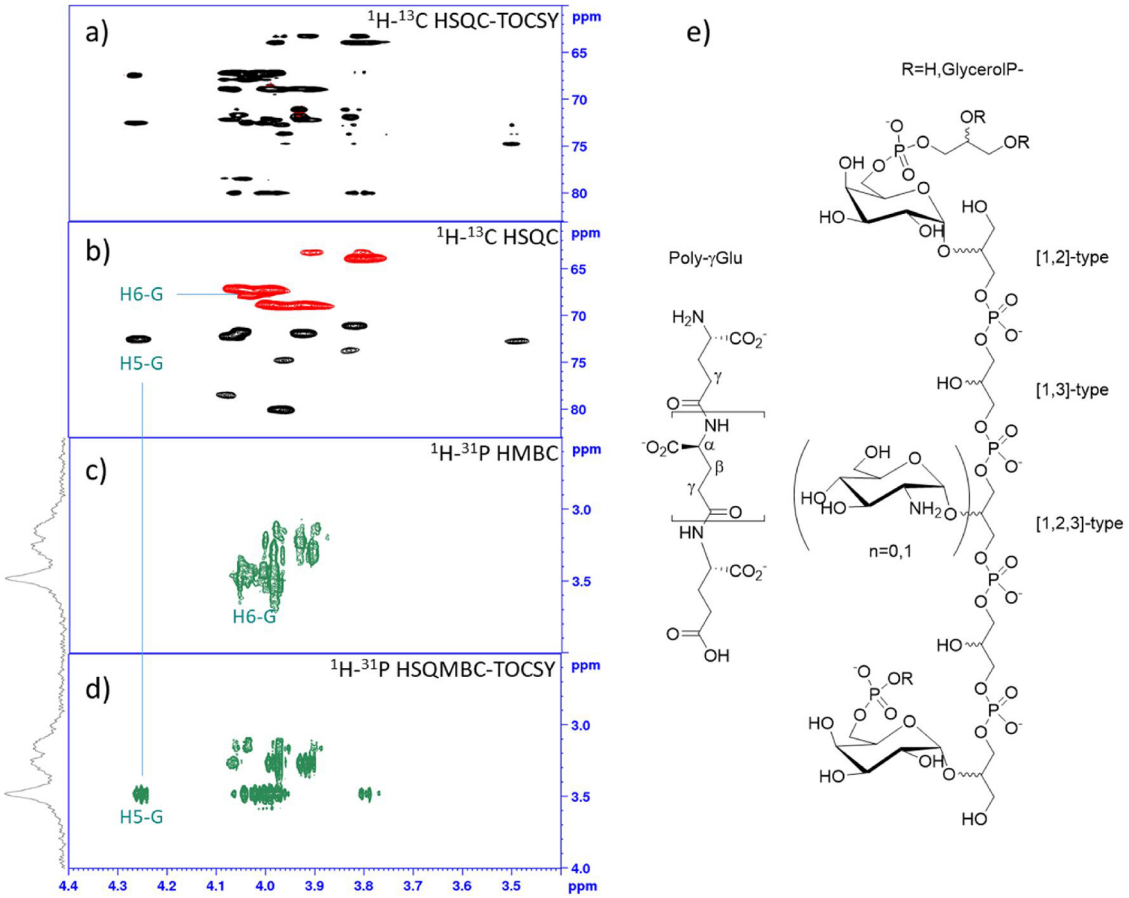

Fig. 3. Nuclear magnetic resonance (NMR). Different heteronuclear 2D experiments were employed to determine the composition and structure of the exopolymer EPSp. a) ^{1}H-^{13}C HSQC-TOSCY, b) ^{1}H-^{13}C HSQC edited, c) ^{1}H-^{31}P HMBC, and d) ^{1}H-^{31P} HSQMBC-TOCSY. Signals corresponding to H5/C5 and H6/C6 cross peaks of Gal are labelled in spectra b), c), and d), assessing the presence of phosphate at Gal O6. e) Proposed idealized structures of the molecular components of the sample.

EPSp on viral infection was evaluated either by immunofluorescence, flow cytometry or quantification of viral production. Viral titer was quantified by an endpoint dilution assay determining the 50 % tissue culture infective dose ($TCID_{50}$) in Vero cells. Each experiment was conducted thrice.

2.13. Viral assays

To investigate dose dependent viral infections, the recombinant HSV-1 (KOS) gL86 was used which expresses beta-galactosidase upon entry into cells (Yakoub et al., 2014). Vero cells plated in 96-well tissue culture dishes were infected at a m.o.i. of 10 with HSV-1 gL86 treated or mock-treated with two-fold serial dilutions of EPSp at concentrations of 6.25, 12.5, 25 and 50 μg/mL. This was prepared following the method described in Section 2.12 and adjusted to obtain the desired concentration. After 6 h p.i., the beta-galactosidase activity was analyzed at 410 nm in a microplate reader.

The effect of the EPSp on different HSV-1 infected cell lines was also analyzed. Several adherent and non-adherent cell lines were chosen: human HOG, Hela, Jurkat and Mewo cells. These were prepared and evaluated following the methodology described in the Section 2.12.

The effect of the EPSp on different viruses was investigated in Section 2.11. The cells were prepared as described in Section 2.12 except for PRV which had an increased base dosage of 10 μg/mL. For dosage comparison purposes, HSV-2 and PRV infected cells were treated with an additional 2-fold dose. For MVM and VSV, there were additional 5-fold and 4-fold dosages respectively.

2.14. Immunofluorescence microscopy

Cells grown on glass coverslips were fixed in 4 % paraformaldehyde for 20 min and rinsed with PBS. Then cells were permeabilized with 0.2 % Triton X-100, rinsed and incubated for 30 min with 3 % bovine serum albumin in PBS with 10 % human serum (only for herpes, to block the HSV-1-induced IgG Fc receptors). For double and triple-labeled immunofluorescence analysis, cells were incubated for 1 h at room temperature with the appropriate primary antibodies, rinsed several times and incubated at room temperature for 30 min with the relevant fluorescent secondary antibodies. Herpes antibodies were incubated in the presence of 10 % human serum. Controls to assess labeling specificity included incubations with control primary antibodies or omission of the primary antibodies. After thorough washing, coverslips were mounted in Mowiol. Images were obtained using an LSM510 META system (Carl Zeiss) coupled to an inverted Axiovert 200 microscope. Processing of confocal images was made by FIJI-ImageJ software.

2.15. Flow cytometry analysis

To perform FACS analysis, cells were dissociated by incubation for 1 min in 0.05 % trypsin/0.1 % EDTA (Invitrogen) at room temperature and washed and fixed in 4 % paraformaldehyde for 15 min. Then, cells were rinsed and resuspended in PBS. Cells were analyzed using a FACSCalibur Flow Cytometer (BD Biosciences).

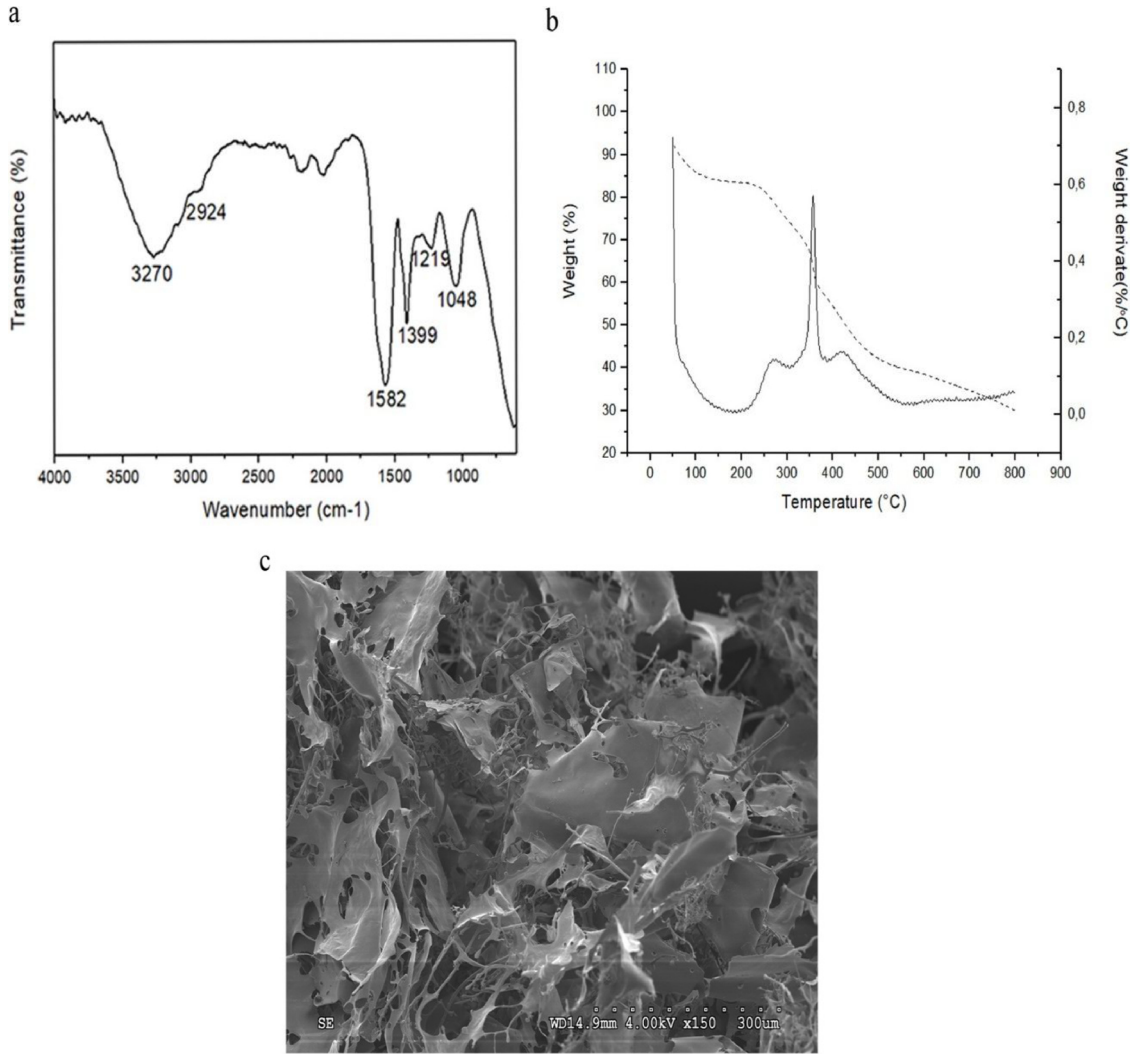

Fig. 4. ATR-FTIR spectra, thermal analysis and ultrastructural characterization of the exopolymer EPSp. a) ATR-FTIR spectra. b) Thermogravimetric analysis and DSC thermogram. c) Scanning electron micrographs.

2.16. In vivo toxicity evaluation of EPSp

To evaluate the toxicity of the EPSp produced by *B. licheniformis* IDN-EC *in vivo,* the Balb/c mouse model was used. Twenty male Balb/c mice (21–27 days) were purchased from Charles River Laboratories España and maintained at the Animal Facility of the Centro de Biología Molecular Severo Ochoa (CBMSO, CSIC-UAM, Madrid, Spain). After 2 weeks of acclimation, mice were randomly distributed in 4 cages of 5 individuals and mock-inoculated or inoculated intraperitoneally with 100 µl of different concentrations of EPSp (6, 60 and 600 µg per animal) diluted in isotonic saline solution (NaCl 0.9 % w/v) from FisioVet (B. Braun VetCare, Barcelona, Spain). The control consisted of 100 µl of the same saline solution. After injection of the acute dose of EPSp, mice were allowed free access to food and water and monitored daily for morbidity, mortality and behavioral changes. At day 14, mice were sacrificed by CO_2 and exsanguinated by cardiac puncture to obtain whole blood, in order to analyze their blood profiles and counts. Several parameters were analyzed to monitor renal, hepatic and immunologic basic profiles. For the biochemical analyses, urea, total protein, alanine aminotransferase (ALT) and bilirubin levels were studied. For hematologic analysis, the percentage of lymphocytes and segmented neutrophils was measured, as well as the WBCs count. The body weight gain from the day 0 (inoculation) to the day 14 (sacrifice) was also quantified, to exclude a weight loss or failure to gain weight that would be indicative of toxicity.

2.17. Statistical analysis

Student's *t*-test was used to determine differences between groups. All data are represented as mean ± standard deviation.

2.18. Ethics statement

This study was carried out in strict accordance with the European Commission legislation for the protection of animals used for scientific purposes (directives 86/609/EEC and 2010/63/EU). Mice were maintained under specific pathogen-free conditions at the CBMSO (CSIC-UAM) animal facility. The protocol for the treatment of the animals was accepted by the "Comité de Ética de la Investigación" of the Universidad Autónoma of Madrid, Spain and approved by the "Consejería General del Medio Ambiente y Ordenación del Territorio de la Comunidad de Madrid" (PROEX 148/15). Animals had unlimited access to food and water, and at the conclusion of the studies they were euthanized in a CO_2 chamber, with every effort made to minimize their suffering, followed by exsanguination by cardiac puncture to obtain whole blood.

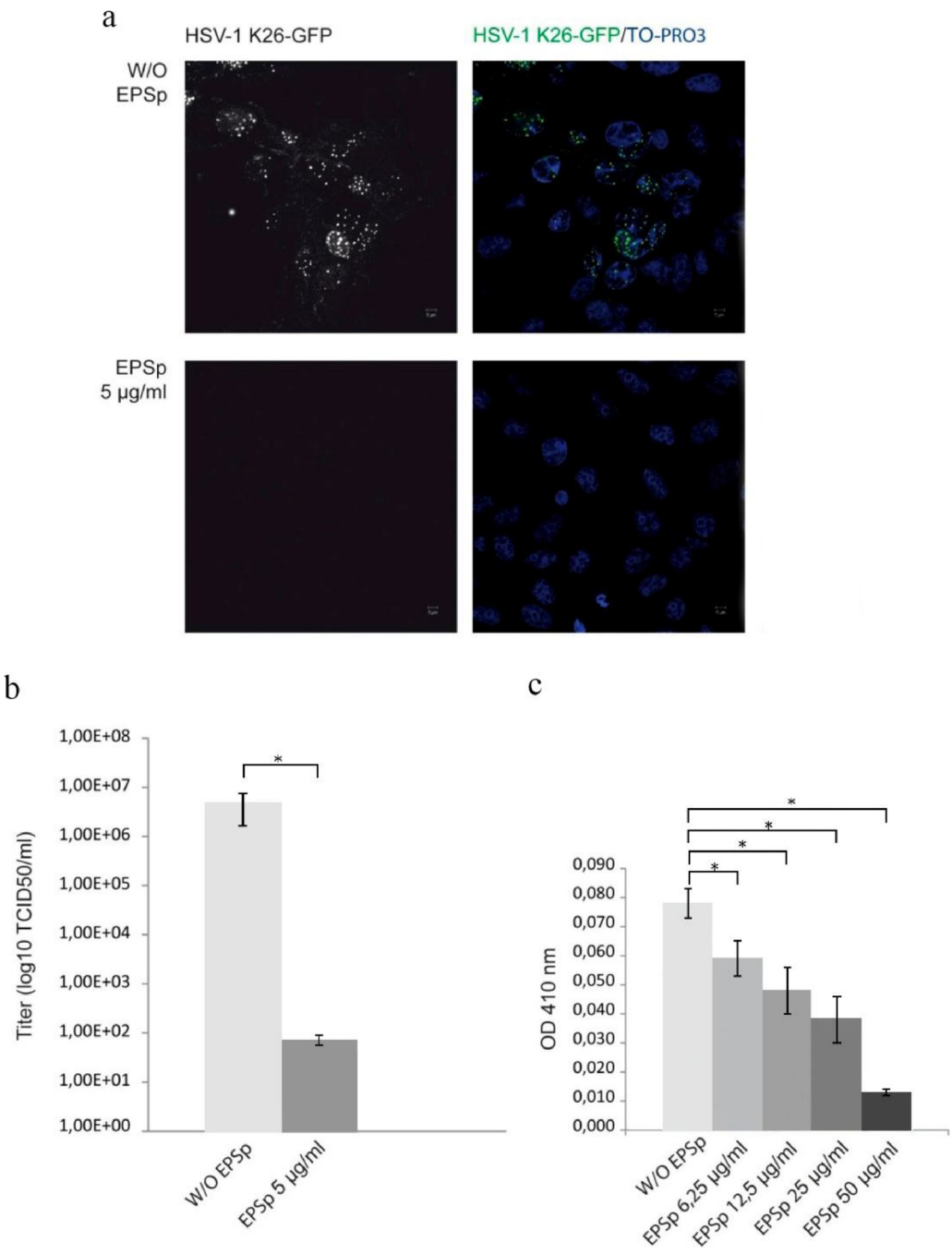

Fig. 5. Exopolymer EPSp extracted from *B. licheniformis* IDN-EC on HSV-1 infection of Vero cell lines. a) Immunofluorescence images of cells show the GFP signal associated to HSV-1 K26. b). Progeny virus was titrated 24 h p.i. to determine the 50 % tissue culture infective dose ($TCID_{50}$)/mL. Histogram shows the viral production cells infected with the control virus (W/O) and the EPSp treated virus (EPSp). c) Histogram shows HSV-1 gL86 pre-treated and the control with two-fold serial dilutions of EPSp 1 mg/mL, at final concentrations of 6.25, 12.5, 25 and 50 µg/mL. After 6 h p.i., the beta-galactosidase activity at 410 nm was analyzed using a microplate reader. (Scale bar = 5 µm, n = 3, * $p < 0.05$).

3. Results

3.1. Biodegradation, cell growth, pH, and EPS production

The growth of *B. licheniformis* IDN-EC, medium biodegradation, pH values and exopolymer production (EPS) at 45 °C, are shown in Fig. 1a. Cellular growth peaked (9.35 log cfu / ml) after 30 h. In this moment, the strain completely biodegraded the glucose as a carbon source. The maximum production of EPS, 60 mg/ L, occurred after 42 h. During the process no acute pH descent was detected, as the acidification of the medium was very low (from pH 7 to just 6.6).

3.2. Characterization of exopolymer

The results of the obtained fraction from the purified exopolymer was named as EPSp. This was found to be water soluble and colorless. The mass spectrum of the polymer indicated that it had an approximate molecular weight of 5 kDa (Fig. 1b). HLPC analysis of EPSp, showed that this was formed by α-D-galactose and α-D-glucosamine with a molar ratio of 3:1. It had lack of glucuronic acid.

The NMR analysis (Table 1 and Figs. 2 and 3) showed the presence of three groups of signals and two different types of molecules with different molecular sizes. The first one is a saccharide as observed in the ^{1}H-NMR spectrum where two anomeric protons can be distinguished, with J couplings of 3.5 and 3.9 Hz, indicative of α type linkages.

However, there are additional signals, below 3 ppm, which do not correspond to a sugar and that are compatible with a peptide, mostly composed by aliphatic amino acid side chains. Diffusion Ordered NMR experiments (DOSY) showed the existence of two different molecules with different diffusion coefficients and therefore, distinct molecular weights (Fig. 2a).

The peptide component shows a typical $-CH(\alpha)-CH_2(\beta)-CH_2(\gamma)$

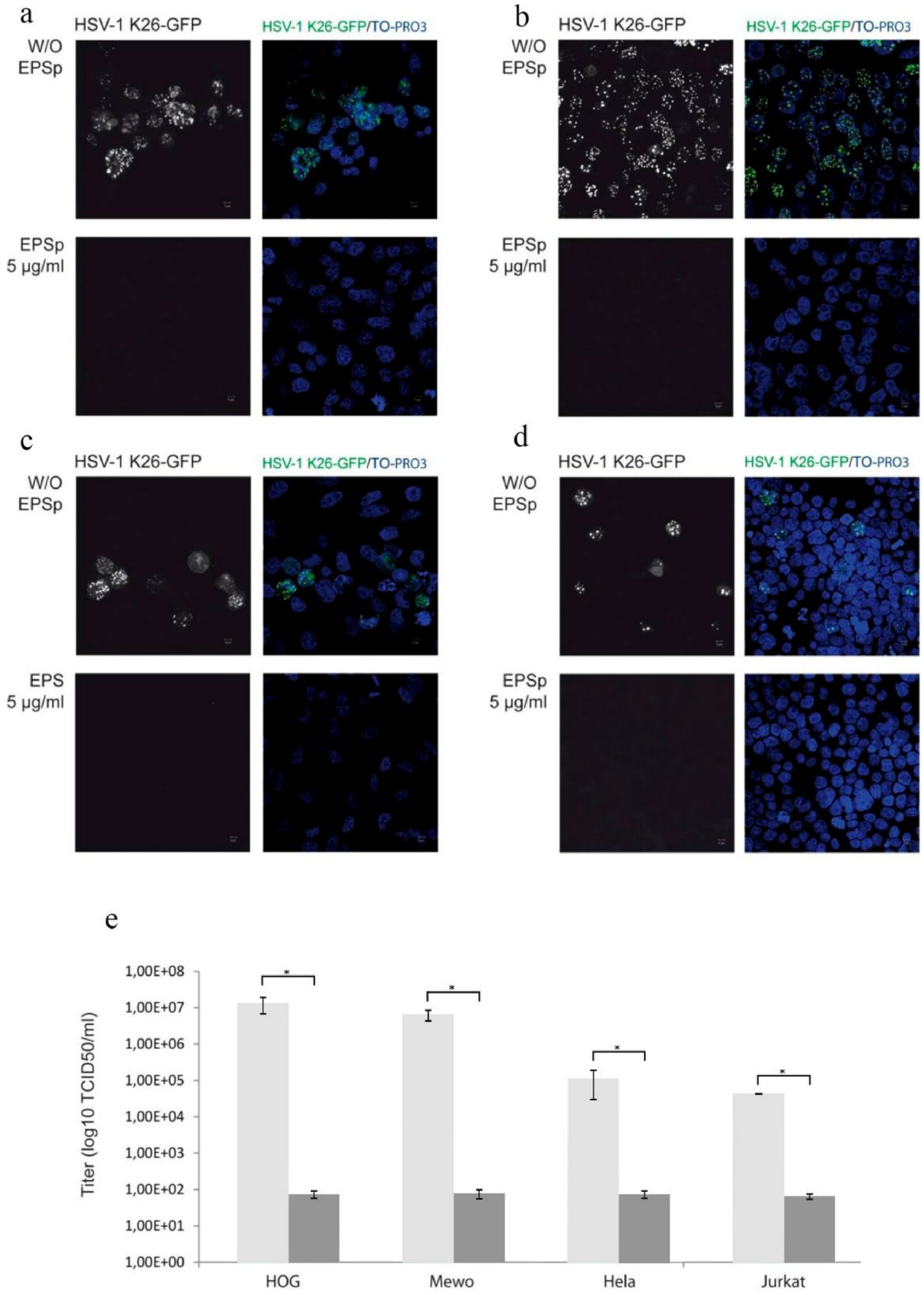

Fig. 6. Effect of exopolymer EPSp extracted from *B. licheniformis* IDN-EC on HSV-1 infection of human cell lines. Immunofluorescence images show the GFP signal associated to HSV-1 K26 in a) HOG, b) Mewo, c) Hela, and d) Jurkat cells. e) Progeny virus was titrated 24 h p.i. to determine the 50 % tissue culture infective dose (TCID50)/mL. Histogram shows the viral production of HOG, Mewo, Hela and Jurkat cells infected with the control virus (W/O) and the EPSp treated virus (EPSp). (Scale bar = 5 µm, n = 3, * $p < 0.05$).

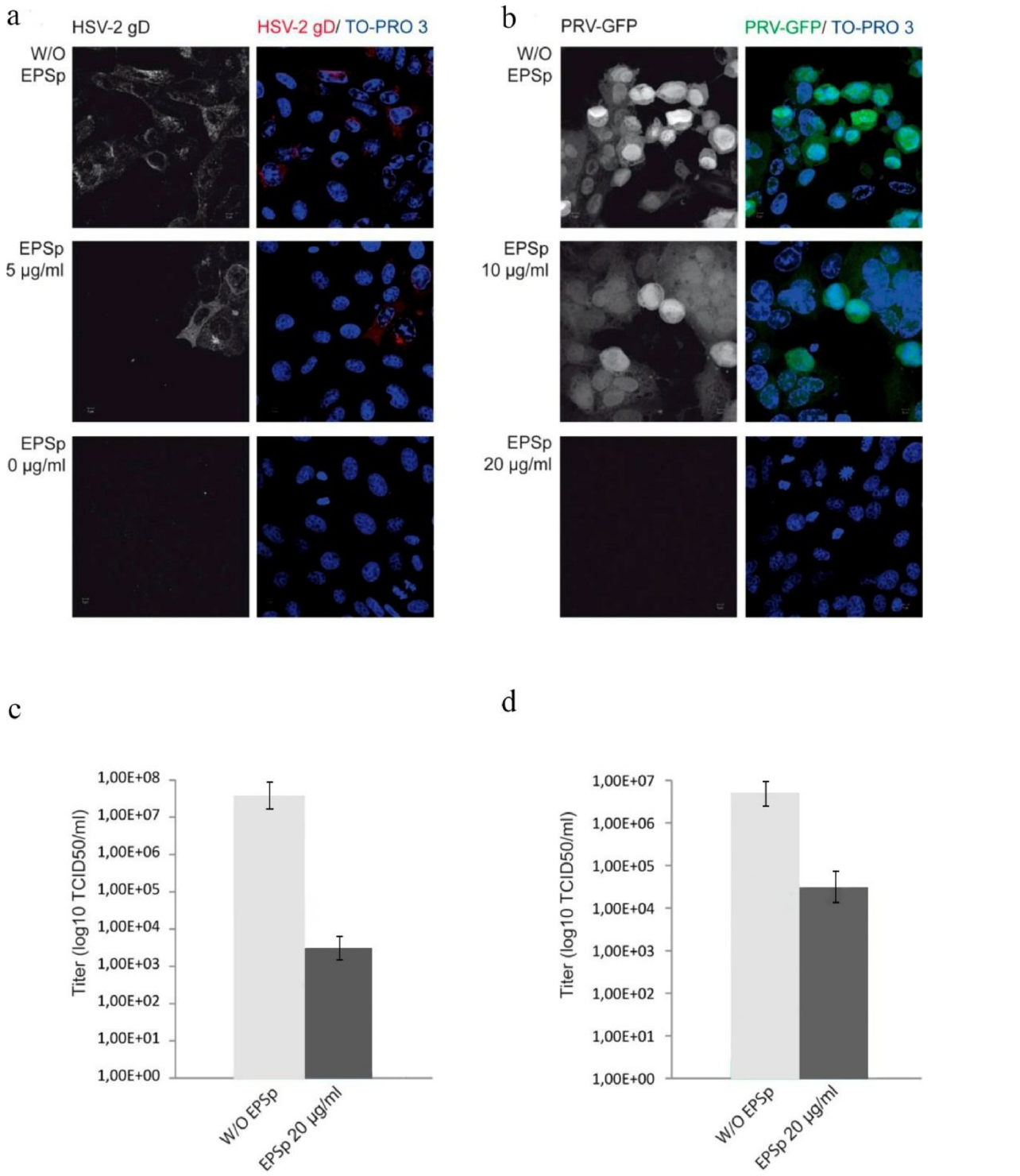

Fig. 7. Exopolymer EPSp extracted from *B. licheniformis* IDN-EC on HSV-2 and PRV-GFP infection of Vero cell line. Immunofluorescence images show a) The monoclonal anti-HSV gD b) GFP signal associated to PRV-GFP in Vero cells. c-d) Histogram shows the viral production cells infected with HSV-2 and PRV-GFP XGF-N for both the control virus (W/O) and the EPSp treated virus (EPSp). Both were treated with same doses EPSp (20 µg/mL) showed a decrease of about 4 and 2 orders of magnitude respectively. (Scale bar = 5 µm n = 3 p < 0.05).

pattern, as determined by COSY and HSQC-edited experiments. Both CH(α) and CH_2(γ) signals correlated with carbonyl signals in the ^{1}H-^{13}C HMBC experiments, at δ 181 and 178 ppm respectively. The γ-linkage of the Glu chain was determined by comparison with the previously described product (Kino, Arai, & Arimura, 2011). Thus, the peptide component could be identified as polyglutamic acid (γ-PGA), which displayed the highest molecular weight.

Regarding the carbohydrate-containing molecule, the detailed analysis was based on the combination of COSY, HSQC, HSQC-TOCSY and 1D-selective TOCSYs experiments (Fig. 3). This protocol allowed identifying the two constituent sugar residues. The signals for the major component showed a typical Gal pattern: The 1D-selective TOCSY experiments from the anomeric proton demonstrated the complete H1-H2-H3-H4 spin system, which is stopped at H4 due to the small H4-H5

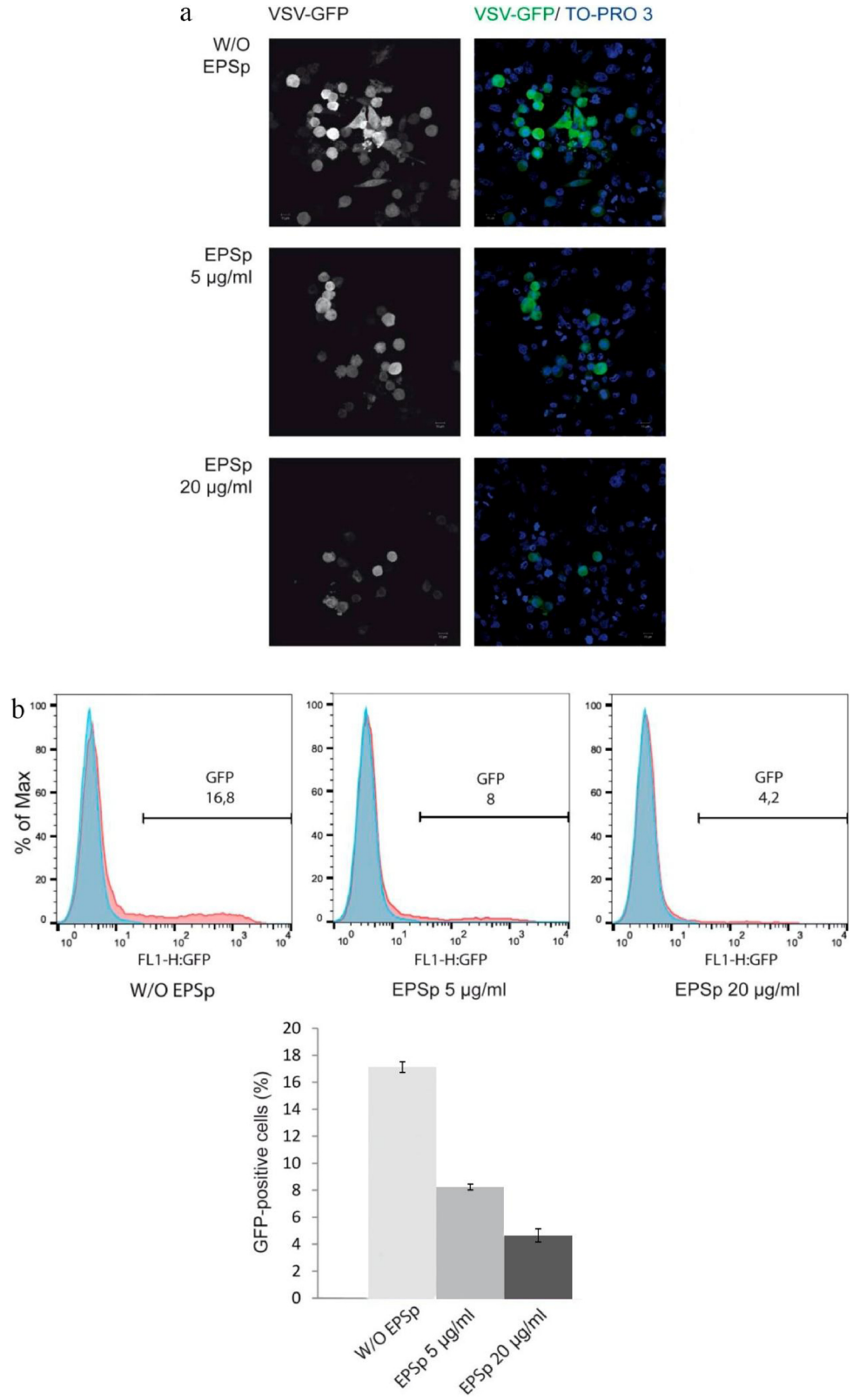

Fig. 8. Effect of exopolymer EPSp extracted from *B. licheniformis* IDN-EC on VSV-GFP infection of Hela cell line. a) Immunofluorescence images of cells show the GFP signal associated to VSV -GFP b) Flow cytometry analysis and histogram showed the fold reduction. The control virus (W/O) and the EPSp treated virus (EPSp). (Scale bar = 10 µm, n = 3 $p < 0.05$).

coupling. This behavior is typical for Gal moieties. Moreover, the ^{13}C chemical shift for C-6 indicated that this OH position was substituted. As observed in the ^{1}H-^{31}P HMBC and HSQCMBC-TOCSY experiments, phosphorylation of Gal sugar moiety at position 6 was confirmed due to the TOCSY correlation of this signal with Gal-H5 position.

The minor component showed a drastically different coupling pattern in the 1D-selective TOCSY, with typical glucose-type couplings: large vicinal ^{1}H-^{1}H J values. In this case, the position C2 in the HSQC

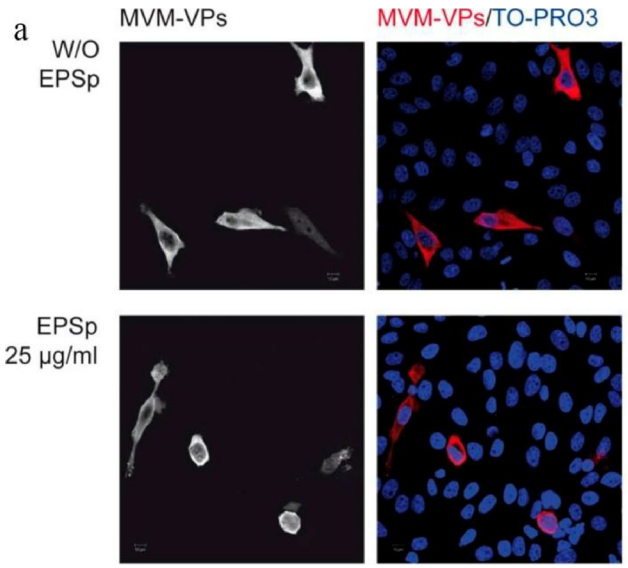

Fig. 9. Effect of exopolymer EPSp extracted from *B. licheniformis* IDN-EC on MVM infection of Hela cell line. a) Immunofluorescence images of cells with the anti-VPs MVM polyclonal antibody followed by an Alexa-555 donkey anti-rabbit secondary antibody. b) Histogram shows the percentage of cells infected with the control virus (W/O) and the EPSp treated virus (EPSp). (Scale bar = 10 µm, n = 3 $p < 0.05$).

showed the typical chemical shift of a carbon attached to a nitrogen atom, instead of oxygen. Since no methyl signals for a putative acetyl group were evidenced in the regular ^{1}H or in the HSQC or in the HMBC spectra, the minor component was identified as an αGlucosamine residue (αGlcN). Indeed, in the HSQC spectra small signals that could belong to methyl groups were identified. However, they only displayed 15 % of the intensity of that expected for a methyl acetate with respect to those belonging to the H1C1 or H2C2 signals of the minor component in the same spectrum. Given that the intensities of the methyl groups are usually magnified thanks to its fast motion features, the presence of N-acetylation should be basically negligible.

In addition to these monosaccharide moieties, NMR signals for glycerol esters were identified with different substitution patterns. From HSQC-edited and HSQC-TOCSY experiments, three CH and four CH_2 glycerol signals were identified. The substitution was deduced from the analysis of the ^{13}C chemical shifts, which allowed differentiating one unsubstituted signal for each group. From the TOCSY correlations it was possible to establish three different substitution patterns in the glycerol subunit: at 1-2 (one OH free, terminal position of the chain), 1-3 and 1-2 -3 OHs (internal positions of the chain). 1D-selective NOESY experiments from both anomeric positions allowed correlating the GlcN H1 to the position 2 of the 1-2 -3 substituted glycerol moiety and the Gal H1 signal to the position 2 of the 1-2 substituted unit. This structure was fully compatible with other poly glycerol phosphates as previously described (Tul'skaya, Vylegzhanina, Streshinskaya, Shaskov, & Naumova, 1991).

With this information it is proposed that the composition of the major products of the sample is the following.

- A long polyglutamic acid with the largest molecular weight.
  A polyglycerol phosphate chain O-substituted with αGal moieties at terminal positions and further modified with $\alpha GlcNH_2$. Given the approximate $\alpha Gal/\alpha GlcNH_2$ 3:1 M ratio and considering that the αGal is at the terminal position, some chains do not display $\alpha GlcNH_2$ units. This can be identified as a teichoic acid polysaccharide.The FT-IR spectroscopic analysis was applied to disclose the polar bonds and the different atom vibrations of the molecules. The results showed (Fig. 4a) the presence of the characteristic bands for poly glutamic acid (γ-PGA) (Mohanraj et al., 2019). The IR spectra of the EPSp of *B. licheniformis* IDN-EC exhibited a broad peak at around 3270 cm^{-1} (range 3600 − 3200 cm^{-1}) for O—H stretching vibration and the peak at 2924 cm^{-1} was associated to an amine group (Prado-Fernández, Rodríguez-Vázquez, Tojo, & Andrade, 2003). The peak at 1582 cm^{-1} was associated to the deformation vibration of an amide group (Sardari et al., 2017). The band at 1399 cm^{-1} was assigned to the group C═O whereas the peak at 1052 $cm^{-1}$was associated to the C—N group. On the other hand, polyphosphate groups were assigned to the presence of characteristic bands at 1219 cm^{-1}, (range 1200 − 900 cm^{-1}), (Grunert et al., 2018) this belonged to the teichoic acid polysaccharide.

Thermogravimetric analysis (TGA) was used to investigate the thermal stability in the inert atmosphere of EPSp obtained from *B. licheniformis* IDN-EC. The EPSp degradation process took place by reduction of average molecular mass weight. The decomposition of the exopolymer started at 242.4 °C and 36 % of weight loss was observed at 357.41 °C. The differential scanning calorimetry (DSC) (Fig. 4b) for EPSp showed exothermic peak for crystallization temperature (Tc) at 272.66 °C and the other two peaks formelting temperatures at Tm1 = 356.79 °C and Tm2 = 423.90 °C. The EPSp was highly crystalline. Therefore, it was a notably thermostable biopolymer. The morphology of the EPSp obtained from *B. licheniformis* IDN-EC was studied using scanning electron microscopy (SEM) (Fig. 4c). A three-dimensional structure was observed with structural units in the form of thin scales of different sizes intertwined with fine fibers, resulting in a natural scaffold structure.

3.3. Effect of EPSp on herpesvirus infection

The antiviral activity of the exopolymer was assessed using the procedures described in Section 2.12. The effects of the EPSp on the HSV-1 K2GFP infection of Vero cells are shown in Fig. 5. The immunofluorescence assays showed an almost complete disappearance of the GFP signal in cells infected with EPSp-treated virus at 24 h p.i. with a 5 µg/mL dose (Fig. 5a). To quantify the effect of exopolymer on viral yield, progeny virus was titrated to determine the $TCID_{50}$/mL. After 24 h p.i., viral yield in Vero cells infected with EPSp-treated virus decreased around 5 orders of magnitude compared to cells infected with mock-treated virus, to become practically undetectable (Fig. 5b).

To investigate whether the decrease in viral yield was due to a decrease in viral entry, Vero cells were infected with the recombinant HSV-1 (KOS) gL86 and treated or mock-treated with two-fold serial dilutions of EPSp as described in Materials and Methods (Viral entry section). After 6 h p.i., the beta-galactosidase activity finding a significant ($p < 0.05$) dose dependent decrease of absorbance in cells treated with EPSp (Fig. 5c), compared to the control mock-treated cells.

Experiments performed with the rest of cell lines, HOG (Fig. 6a),

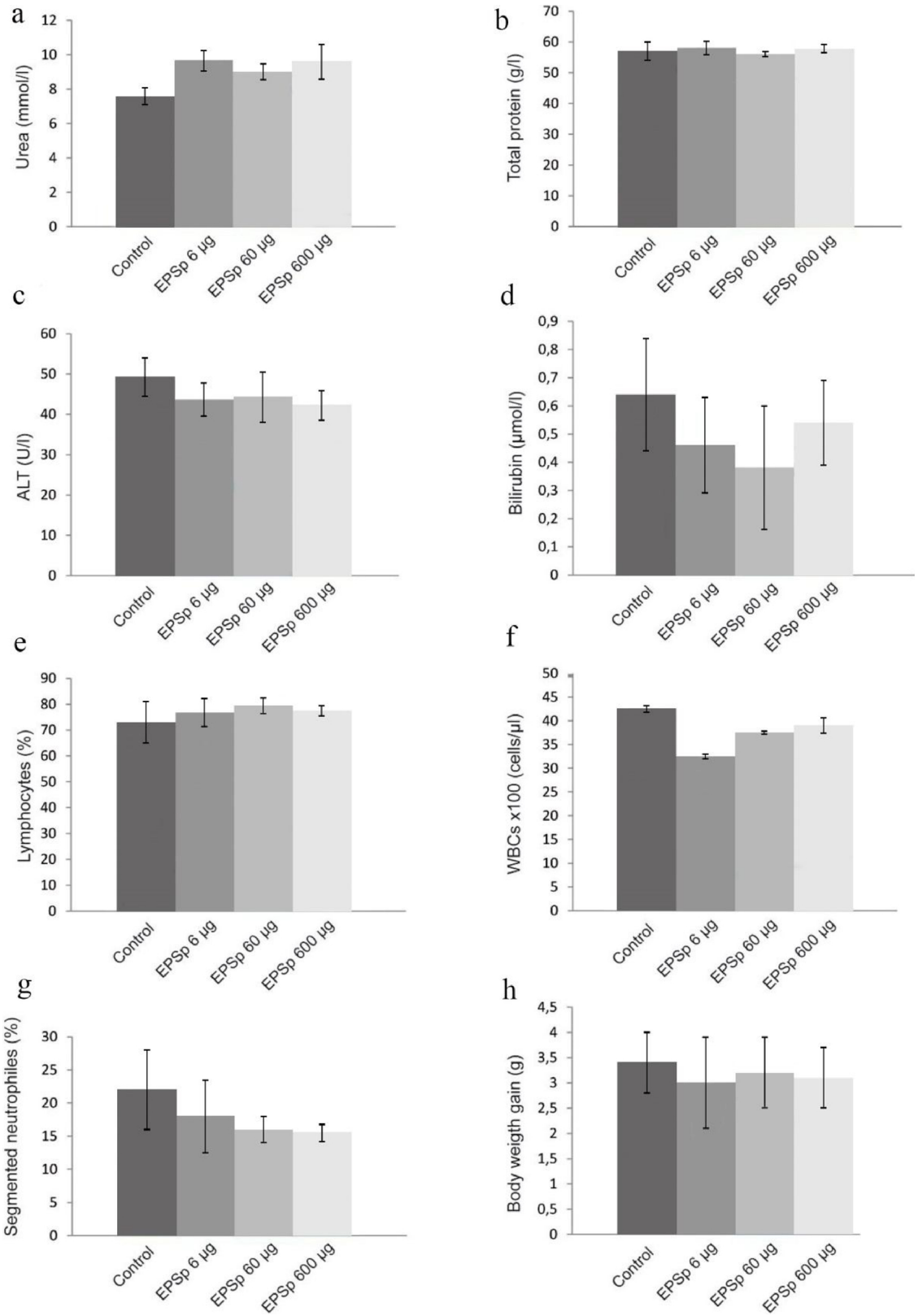

Fig. 10. *In vivo* toxicity evaluation of EPSp. Twenty male Balb/c mice were randomly distributed in cages of 5 individuals and inoculated or mock-inoculated intraperitoneally with 100 µl of ten-fold concentrations of EPSp diluted in NaCl 0.9 % w/v: 6, 60 and 600 µg of EPSp per animal. At day 14, mice were sacrificed and whole blood was obtained by cardiac puncture. For the biochemical analyses, urea (a), total protein (b), ALT (c) and bilirubin (d) levels were tested. For hematologic study, the percentages of lymphocytes (e), WBCs count (f) and segmented neutrophils (g) were analyzed. The body weight gain was also monitored (h). Control: 100 µl of NaCl 0.9 % w/v per animal. (ALT: alanine aminotransferase; WBC: white blood cells).

Mewo (Fig. 6b), Hela (Fig. 6c) and Jurkat (Fig. 6d), showed similar results: immunofluorescence assays showed a drastic decrease of GFP signal in cells infected with EPSp-treated virus at 24 h p.i. and, in addition, viral progeny decreased around 4–5 orders of magnitude (depending on the infectivity of the cell lines) in cells infected with EPSp-treated virus compared to the control.

To analyze whether the results previously shown could be extrapolated to other herpesviruses, Vero cells were infected with HSV-2 and PRV-GFP XGF-N (Fig. 7) at a m.o.i. of 0.5. Infection with HSV-2 (Fig. 7a) treated with EPSp at 5 μg/mL showed only a moderate decrease compared to mock-treated control. However, with HSV-2 treated with EPSp at 10 μg/mL, infection drastically decreased. On the other hand, infections with PRV-GFP XGF-N at an m.o.i. of 0.5 yielded similar results at 24 h p.i., although the effect of EPSp on PRV infection was less pronounced (Fig. 7b). Thus, infection with PRV-GFP XGF-N treated with EPSp at 10 μg/mL did not caused any observable effect compared to mock-treated control and, to inhibit infection, a dose of EPSp at 20 μg/mL was needed (Fig. 7b). Similarly, quantification of viral production with HSV-2and PRV-GFP XGF-N, both treated with same doses EPSp (20 μg/mL) showed a decrease of about 4 and 2 orders of magnitude respectively (Fig. 7c and d).

3.4. Effect of EPSp on other enveloped (VSV) and non-enveloped (MVM) viruses

To analyze whether the results above described could be extrapolated to another enveloped virus, cells were infected with VSV-GFP at a m.o.i. of 0.5. As shown in Fig. 8a, the decrease of VSV infection was most noticeable with an EPSp dose of 20 μg/mL. In addition, flow cytometry analysis showed a 4-fold reduction in the viral-GFP signal of cells infected with VSV-GFP treated with EPSp 20 μg/mL when compared to non-treated control, and 2-fold reduction when compared to the 5 μg/mL EPSp treatment (Fig. 8b).

Finally, the EPSp was tested on a non-enveloped virus, MVM. Hela cells were infected with EPSp treated or mock-treated MVM. After 24 h p.i., no change in viral-associated signal was observed in the cells as shown by the immunofluorescence images and the accompanying histogram quantification (Fig. 9a and b).

3.5. In vivo toxicity evaluation of EPSp in mice

Twenty male Balb/c mice were mock-inoculated or inoculated with different single doses of the EPSp Section 2.16. Several parameters were analyzed. For the biochemical analysis, levels of urea (Fig. 10a), total protein (Fig. 10b), alanine aminotransferase (ALT) (Fig. 10c) and bilirubin (Fig. 10d) were measured. For hematologic analysis, the percentage of lymphocytes (Fig. 10e), the white blood cells (WBCs) count (Fig. 10f) and segmented neutrophils (Fig. 10g) were evaluated. For 14 days there were no significant changes in any of the parameters between the control and experimental groups. No toxic signs were observed such as hypothermia, weakness, diarrhea or ataxia. There were also no signs of acute pain, distress or weight loss.

4. Discussion

The aim of this work was to isolate and characterize a natural exopolymer produced by *B. licheniformis* IDN-EC strain and to evaluate its role as a potential antiviral agent.

During the polymer production process (Fig. 1a), essential factors like the carbon and nitrogen sources, aeration, agitation and medium pH were controlled. These factors can have an important effect on the quantity and quality of the polymer (Kongklom, Luo, Shi, & Pechyen, 2015). The characterization assays conducted on the produced polymer (EPSp) (Figs. 2, 3 and 4a) identified two components: Poly-γ-glutamic acid (γ-PGA) and an extracellular teichoic acid (EC-TA).

γ-PGA is an anionic polymer due to the presence of carboxylic groups that can interact electrostatically with positive charges (Pereira et al., 2017). These have been found to be secreted by different species of the *Bacillus* genus, such as *B. licheniformis* and *B. subtilis* (Bajaj & Singhal, 2011) and have been described to have antiviral properties but this is only for high molecular weights (Lee et al., 2013).

The teichoic acid polysaccharide was composed of polyphosphate and was substituted at the 2-position of glycerol residues with a αGal, $\alpha GlcNH_2$. In addition to this, the αGal O-6 position was substituted by a phosphate group. This polysaccharide can be identified as a teichoic acid due to the presence of the polyphosphate compound. A teichoic acid is a polysaccharide that is only produced by gram-positive bacteria. An unusual trait of this teichoic acid is that it is extracellular (EC−TA) since this type of TA has only been described in a limited number of species (Xiao & Zheng, 2016) (Jabbouri & Sadovskaya, 2010). As well as being extracellular, this TA was also found to be atypical due to the nature of its charges (Weidenmaier & Peschel, 2008). These only contain negatively charged phosphate groups and positive charges are absent, this has only been previously described for *Bacillus subtilis*. In addition to this, the substitution by phosphate groups in the O-6 position of the αGal would increase the electrostatic properties of the EC−TA. It has been found with other compounds that when the αGal O-6 position is substituted with negative charges such as sulphates, there is an increase in the antiviral capability of these (Ghosh et al., 2009). The significant negative overall charge of the two polymer components of the EPSp (the γ-PGA and the EC−TA) would have a synergy effect thus increasing the antiviral effect of the polymer.

The molecular weight of the EPSp, (5 kDa) (Fig. 1b) is similar to the pentosan polysulphates (3 kDa), and dextran sulphates (5 kDa) (Mbemba, Chams, Gluckman, Klatzmann, & Gattegno, 1992). These compounds with a high number of negative charges have previously been described as highly effective in inhibiting the replication of enveloped viruses and ineffective against non-enveloped viruses (Wang, Wang, & Guan, 2012). As well as a low molecular weight, the morphology of the polymer can ease contact. The natural scaffold of the *B. licheniformis* IDN-EC EPSp presented a non-uniform morphology (Fig. 4c). This is especially relevant as a non-uniform surface could promote viral contact, in a similar way to cell adhesion. This would in turn favor the polymer-virus interaction and significantly increase the efficiency of antiviral activity (De Colli et al., 2012).

The antiviral capability of this EPSp was tested by infecting Vero cells with HSV-1 K26-GFP and varying the dose and cell type. HSV-1 was pretreated with the EPSp prior to cell infection. The titration results and the immunofluorescence images confirmed that the EPSp has a virucidal dose-dependent effect in the viral entry as the EPS was more effective with larger doses (Fig. 5) (Schnitzler, Schneider, Stintzing, Carle, & Reichling, 2008). The effectiveness against different cell lines also suggested that the EPS could inhibit the first step of viral infection by preventing entry through both endocytosis and fusion (Figs. 5 and 6).

The antiviral capability of this EPSp was also tested on both enveloped (herpesviruses and VSV) and non-enveloped (MVM) viruses. The obtained differences in inhibition efficiency of the EPSp among the herpesviruses (HSV-1 (5 μg/mL) > HSV-2 (10 μg/mL) > PRV (20 μg/mL) (Figs. 5 and 7) and VSV, (20 μg/mL) (Fig. 8) could be due to the different capabilities of the viral glycoproteins to establish unspecific electrostatic bonds. HSV-1 has been found to be most effective in establishing this type of bonds with the cells that it infects (Ho, Jeng, Hu, & Chang, 2000). The EPSp did not present any antiviral effects against MVM (Fig. 9). This suggests that the antiviral properties might be a universal phenomenon against enveloped viruses which would make the EPSp a potential antiviral treatment against other enveloped viruses such as SARS-CoV-2. Furthermore, the *in vivo* assay of the EPSp in mice showed no signs of toxicity (Fig. 10).

5. Conclusion

This study demonstrates that the exopolymer produced by B. *licheniformis* IDN-EC was composed of Poly-γ-glutamic acid and a teichoic acid. The negative charge content increased the electrostatic properties of the EPSp. This meant that the EPSp was highly effective as an antiviral treatment against a group of human and animal enveloped viruses. This further suggests that the novel EPSp could be a good candidate for further studies in cell cultures with other enveloped viruses. The *in vivo* results also imply that there is a potential application in the pharmaceutical industry as a prophylactic therapeutic biomolecule. Future tests in animal models would establish its efficacy *in vivo* against enveloped viral infection.

CRediT authorship contribution statement

E. Sánchez-León: Formal analysis, Investigation, Resources, Writing - original draft. **R. Bello-Morales:** Formal analysis, Investigation, Resources, Writing - original draft. **J.A. López-Guerrero:** Funding acquisition. **A. Poveda:** Formal analysis, Resources, Writing - original draft. **J. Jiménez-Barbero:** Formal analysis, Resources. **N. Gironès:** Funding acquisition. **C. Abrusci:** Conceptualization, Formal analysis, Funding acquisition, Methodology, Resources, Supervision, Writing - original draft, Writing - review & editing.

Acknowledgments

We have acknowledged Universidad Autonoma de Madrid, Spain (P. Ref. 905089). We are grateful to the technical staff of the “Servicio Interdepartamental de Investigación (SIdI) de la UAM”. We are grateful to the technical staff of the CBMSO, for their support.

References

Abrusci, C., Pablos, J. L., Corrales, T., López-Marín, J., Marín, I., & Catalina, F. (2011). Biodegradation of photo-degraded mulching films based on polyethylenes and stearates of calcium and iron as pro-oxidant additives. *International Biodeterioration & Biodegradation, 65*(3), 451–459. https://doi.org/10.1016/j.ibiod.2010.10.012.

Alonso, R., Mazzeo, C., Mérida, I., & Izquierdo, M. (2007). A new role of diacylglycerol kinase α on the secretion of lethal exosomes bearing Fas ligand during activation-induced cell death of T lymphocytes. *Biochimie, 89*(2), 213–221. https://doi.org/10.1016/j.biochi.2006.07.018.

Arena, A., Maugeri, T. L., Pavone, B., Iannello, D., Gugliandolo, C., & Bisignano, G. (2006). Antiviral and immunoregulatory effect of a novel exopolysaccharide from a marine thermotolerant Bacillus licheniformis. *International Immunopharmacology, 6*(1), 8–13. https://doi.org/10.1016/j.intimp.2005.07.004.

Ates, O. (2015). Systems biology of microbial exopolysaccharides production. *Frontiers in Bioengineering and Biotechnology, 3*(December), 1–16. https://doi.org/10.3389/fbioe.2015.00200.

Bajaj, I., & Singhal, R. (2011). Poly (glutamic acid) - an emerging biopolymer of commercial interest. *Bioresource Technology, 102*(10), 5551–5561. https://doi.org/10.1016/j.biortech.2011.02.047.

Bello-Morales, R., Crespillo, A. J., Fraile-Ramos, A., Tabarés, E., Alcina, A., & López-Guerrero, J. A. (2012). Role of the small GTPase Rab27a during Herpes simplex virus infection of oligodendrocytic cells. *BMC Microbiology, 12*. https://doi.org/10.1186/1471-2180-12-265.

Birch, J., Van Calsteren, M. R., Pérez, S., & Svensson, B. (2019). The exopolysaccharide properties and structures database: EPS-DB. Application to bacterial exopolysaccharides. *Carbohydrate Polymers, 205*(June 2018), 565–570. https://doi.org/10.1016/j.carbpol.2018.10.063.

De Colli, M., Massimi, M., Barbetta, A., Di Rosario, B. L., Nardecchia, S., Conti Devirgiliis, L., & Dentini, M. (2012). A biomimetic porous hydrogel of gelatin and glycosaminoglycans cross-linked with transglutaminase and its application in the culture of hepatocytes. *Biomedical Materials (Bristol, England), 7*(5), https://doi.org/10.1088/1748-6041/7/5/055005.

Desai, P., & Person, S. (1998). Incorporation of the green fluorescent protein into the herpes simplex virus type 1 capsid. *Journal of Virology, 72*(9), 7563–7568. https://doi.org/10.1128/jvi.72.9.7563-7568.1998.

Donot, F., Fontana, A., Baccou, J. C., & Schorr-Galindo, S. (2012). Microbial exopolysaccharides: Main examples of synthesis, excretion, genetics and extraction. *Carbohydrate Polymers, 87*(2), 951–962. https://doi.org/10.1016/j.carbpol.2011.08.083.

Ghosh, T., Chattopadhyay, K., Marschall, M., Karmakar, P., Mandal, P., & Ray, B. (2009). Focus on antivirally active sulfated polysaccharides: From structure-activity analysis to clinical evaluation. *Glycobiology, 19*(1), 2–15. https://doi.org/10.1093/glycob/cwn092.

Gorbalenya, A. E., Baker, S. C., Baric, R. S., de Groot, R. J., Drosten, C., Gulyaeva, A. A., ... Ziebuhr, J. (2020). The species severe acute respiratory syndrome-related coronavirus: Classifying 2019-nCoV and naming it SARS-CoV-2. *Nature Microbiology*. https://doi.org/10.1038/s41564-020-0695-z (Box 1).

Grunert, T., Jovanovic, D., Sirisarn, W., Johler, S., Weidenmaier, C., Ehling-Schulz, M., & Xia, G. (2018). Analysis of Staphylococcus aureus wall teichoic acid glycoepitopes by Fourier Transform Infrared Spectroscopy provides novel insights into the staphylococcal glycocode. *Scientific Reports, 8*(1), 1–9. https://doi.org/10.1038/s41598-018-20222-6.

Gugliandolo, C., Spanò, A., Maugeri, T., Poli, A., Arena, A., & Nicolaus, B. (2015). Role of bacterial exopolysaccharides as agents in counteracting immune disorders induced by herpes virus. *Microorganisms, 3*(3), 464–483. https://doi.org/10.3390/microorganisms3030464.

Harrison, C. (2020). Coronavirus puts drug repurposing on the fast track. *Nature Biotechnology, 38*(April), 379–381. https://doi.org/10.1038/d41587-020-00003-1.

Ho, T.-C., Jeng, K.-S., Hu, C.-P., & Chang, C. (2000). Effects of genomic length on translocation of hepatitis B virus polymerase-linked oligomer. *Journal of Virology, 74*(19), 9010–9018. https://doi.org/10.1128/jvi.74.19.9010-9018.2000.

Jabbouri, S., & Sadovskaya, I. (2010). Characteristics of the biofilm matrix and its role as a possible target for the detection and eradication of Staphylococcus epidermidis associated with medical implant infections. *FEMS Immunology and Medical Microbiology, 59*(3), 280–291. https://doi.org/10.1111/j.1574-695X.2010.00695.x.

Kino, K., Arai, T., & Arimura, Y. (2011). Poly-α-glutamic acid synthesis using a novel catalytic activity of Rimk from Escherichia coli K-12. *Applied and Environmental Microbiology, 77*(6), 2019–2025. https://doi.org/10.1128/AEM.02043-10.

Kongklom, N., Luo, H., Shi, Z., & Pechyen, C. (2015). Production of poly-γ-glutamic acid by glutamic acid-independent Bacillus licheniformis TISTR 1010 using different feeding strategies. *Biochemical Engineering Journal, 100*, 67–75. https://doi.org/10.1016/j.bej.2015.04.007.

Lee, W., Lee, S. H., Ahn, D. G., Cho, H., Sung, M. H., Han, S. H., & Oh, J. W. (2013). The antiviral activity of poly-γ-glutamic acid, a polypeptide secreted by Bacillus sp., through induction of CD14-dependent type I interferon responses. *Biomaterials, 34*(37), 9700–9708. https://doi.org/10.1016/j.biomaterials.2013.08.067.

Marino-Merlo, F., Papaianni, E., Maugeri, T. L., Zammuto, V., Spanò, A., Nicolaus, B., ... Gugliandolo, C. (2017). Anti-herpes simplex virus 1 and immunomodulatory activities of a poly-γ- glutamic acid from Bacillus horneckiae strain APA of shallow vent origin. *Applied Microbiology and Biotechnology, 101*(20), 7487–7496. https://doi.org/10.1007/s00253-017-8472-5.

Mbemba, E., Chams, V., Gluckman, J. C., Klatzmann, D., & Gattegno, L. (1992). Molecular interaction between HIV-1 major envelope glycoprotein and dextran sulfate. *BBA - Molecular Basis of Disease, 1138*(1), 62–67. https://doi.org/10.1016/0925-4439(92)90152-D.

Mohanraj, R., Gnanamangai, B. M., Ramesh, K., Priya, P., Srisunmathi, R., Poornima, S., ... Robinson, J. P. (2019). Optimized production of gamma poly glutamic acid (γ-PGA) using sago. *Biocatalysis and Agricultural Biotechnology, 22*(October), https://doi.org/10.1016/j.bcab.2019.101413.

Montgomery, R. I., Warner, M. S., Lum, B. J., & Spear, P. G. (1996). Herpes simplex virus-1 entry into cells mediated by a novel member of the TNF/NGF receptor family. *Cell, 87*(3), 427–436. https://doi.org/10.1016/S0092-8674(00)81363-X.

More, T. T., Yadav, J. S. S., Yan, S., Tyagi, R. D., & Surampalli, R. Y. (2014). Extracellular polymeric substances of bacteria and their potential environmental applications. *Journal of Environmental Management, 144*, 1–25. https://doi.org/10.1016/j.jenvman.2014.05.010.

Morro, A., Catalina, F., Sanchez-León, E., & Abrusci, C. (2019). Photodegradation and biodegradation under thermophile conditions of mulching films based on poly (Butylene Adipate-co-Terephthalate) and its blend with poly(Lactic acid). *Journal of Polymers and the Environment, 27*(2), 352–363. https://doi.org/10.1007/s10924-018-1350-0.

Nácher-Vázquez, M., Ballesteros, N., Canales, Á., Rodríguez Saint-Jean, S., Pérez-Prieto, S. I., Prieto, A., ... López, P. (2015). Dextrans produced by lactic acid bacteria exhibit antiviral and immunomodulatory activity against salmonid viruses. *Carbohydrate Polymers, 124*, 292–301. https://doi.org/10.1016/j.carbpol.2015.02.020.

Panosyan, H., Di Donato, P., Poli, A., & Nicolaus, B. (2018). Production and characterization of exopolysaccharides by Geobacillus thermodenitrificans ArzA-6 and Geobacillus toebii ArzA-8 strains isolated from an Armenian geothermal spring. *Extremophiles, 22*(5), 725–737. https://doi.org/10.1007/s00792-018-1032-9.

Pereira, A. E. S., Sandoval-Herrera, I. E., Zavala-Betancourt, S. A., Oliveira, H. C., Ledezma-Pérez, A. S., Romero, J., & Fraceto, L. F. (2017). γ-Polyglutamic acid/chitosan nanoparticles for the plant growth regulator gibberellic acid: Characterization and evaluation of biological activity. *Carbohydrate Polymers, 157*, 1862–1873. https://doi.org/10.1016/j.carbpol.2016.11.073.

Prado-Fernández, J., Rodríguez-Vázquez, J. A., Tojo, E., & Andrade, J. M. (2003). Quantitation of κ-, ι- and λ-carrageenans by mid-infrared spectroscopy and PLS regression. *Analytica Chimica Acta, 480*(1), 23–37. https://doi.org/10.1016/S0003-2670(02)01592-1.

Rehm, B. H. A. (2010). Bacterial polymers: Biosynthesis, modifications and applications. *Nature Reviews Microbiology, 8*(8), 578–592. https://doi.org/10.1038/nrmicro2354.

San Miguel, V., Peinado, C., Catalina, F., & Abrusci, C. (2009). Bioremediation of naphthalene in water by Sphingomonas paucimobilis using new biodegradable surfactants based on poly (ε-caprolactone). *International Biodeterioration & Biodegradation, 63*(2), 217–223. https://doi.org/10.1016/j.ibiod.2008.09.005.

Sardari, R. R. R., Kulcinskaja, E., Ron, E. Y. C., Björnsdóttir, S., Friðjónsson, Ó. H., Hreggviðsson, G.Ó., & Karlsson, E. N. (2017). Evaluation of the production of exopolysaccharides by two strains of the thermophilic bacterium Rhodothermus marinus. *Carbohydrate Polymers, 156*, 1–8. https://doi.org/10.1016/j.carbpol.2016.08.

062.
Schnitzler, P., Schneider, S., Stintzing, F. C., Carle, R., & Reichling, J. (2008). Efficacy of an aqueous Pelargonium sidoides extract against herpesvirus. *Phytomedicine, 15*(12), 1108–1116. https://doi.org/10.1016/j.phymed.2008.06.009.
Tul'skaya, E. M., Vylegzhanina, K. S., Streshinskaya, G. M., Shaskov, A. S., & Naumova, I. B. (1991). 1,3-Poly(glycerol phosphate) chains in the cell wall of Streptomyces rutgersensis var. castelarense VKM Ac-238. *BBA - General Subjects, 1074*(2), 237–242. https://doi.org/10.1016/0304-4165(91)90158-D.
Viejo-Borbolla, A., Muñoz, A., Tabarés, E., & Alcamí, A. (2010). Glycoprotein G from pseudorabies virus binds to chemokines with high affinity and inhibits their function. *The Journal of General Virology, 91*(1), 23–31. https://doi.org/10.1099/vir.0.011940-0.
Wang, W., Wang, S. X., & Guan, H. S. (2012). The antiviral activities and mechanisms of marine polysaccharides: An overview. *Marine Drugs, 10*(12), 2795–2816. https://doi.org/10.3390/md10122795.
Weidenmaier, C., & Peschel, A. (2008). Teichoic acids and related cell-wall glycopolymers in gram-positive physiology and host interactions. *Nature Reviews Microbiology, 6*(4), 276–287. https://doi.org/10.1038/nrmicro1861.
Xiao, R., & Zheng, Y. (2016). Overview of microalgal extracellular polymeric substances (EPS) and their applications. *Biotechnology Advances, 34*(7), 1225–1244. https://doi.org/10.1016/j.biotechadv.2016.08.004.
Yakoub, A. M., Rawal, N., Maus, E., Baldwin, J., Shukla, D., & Tiwari, V. (2014). Comprehensive analysis of herpes simplex virus 1 (HSV-1) entry mediated by zebrafish 3-O-Sulfotransferase isoforms: Implications for the development of a zebrafish model of HSV-1 infection. *Journal of Virology, 88*(21), 12915–12922. https://doi.org/10.1128/jvi.02071-14.
Yim, J. H., Kim, S. J., Ahn, S. H., Lee, C. K., Rhie, K. T., & Lee, H. K. (2004). Antiviral effects of sulfated exopolysaccharide from the marine microalga Gyrodinium impudicum strain KG03. *Marine Biotechnology, 6*(1), 17–25. https://doi.org/10.1007/s10126-003-0002-z.
Yu, Y., Shen, M., Song, Q., & Xie, J. (2018). Biological activities and pharmaceutical applications of polysaccharide from natural resources: A review. *Carbohydrate Polymers, 183*(235), 91–101. https://doi.org/10.1016/j.carbpol.2017.12.009.
Zheng, W., Chen, C., Cheng, Q., Wang, Y., & Chu, C. (2006). Oral administration of exopolysaccharide from Aphanothece halophytica (Chroococcales) significantly inhibits influenza virus (H1N1)-induced pneumonia in mice. *International Immunopharmacology, 6*(7), 1093–1099. https://doi.org/10.1016/j.intimp.2006.01.020.